Nonlinear Wave Loading on Floating Offshore Wind Turbine Platforms

Haoyu Ding[1, 2, 3*], Jun Zang[3], Dezhi Ning[1, 2]
[1]State Key Laboratory of Coastal and Offshore Engineering, Dalian University of Technology, Dalian, China
[2]Dalian Key Laboratory of Offshore Renewable Energy, Dalian University of Technology, Dalian, China
[3]Department of Architecture & Civil Engineering, University of Bath, Bath, UK
*Email: h.ding@dlut.edu.cn

1 INTRODUCTION

Offshore wind turbines operate in challenging and harsh environmental conditions, where environmental loads often dictate design choices. Under extreme wave scenarios, especially for monopile foundations, the total wave loading generally comprises a primary component near the spectral peak and additional higher-order harmonics arising from nonlinear sea-states and wave-structure interactions. These harmonics typically cluster around integer multiples of the fundamental frequency [1]. Based on the insights we found for nonlinear wave loading on monopile foundations between linear and higher-order loading harmonics, we developed a machine learning based Stokes-GP model, trained over a large dataset collected from several phases of experiments and CFD simulations for rapidly predicting nonlinear wave loading on monopiles over a wide range of wave conditions [2], and created SeaSwallowsTools [3], an open-access engineering tool designed for quick prediction of nonlinear wave loading on monopile foundations. Although this tool effectively addresses the nonlinear wave loading on monopile foundations of offshore wind turbines, it is limited to a specific offshore wind turbine foundation type—monopiles.

This research explores the nonlinear wave loading analogies across different floating offshore wind turbine platforms. The phase-decomposition method is employed to isolate individual force harmonics from the overall wave loading, demonstrating its potential feasibility for floating offshore wind turbine platforms in this abstract.

2 PHASE-DECOMPOSITION METHOD

A phase-decomposition approach, used for a bottom-mounted cylinder in [1], effectively isolates individual harmonics. This analysis involves the diffraction of a unidirectional focused incident wave by the structure. Based on the classic Stokes perturbation expansion [4], the inline hydrodynamic load can be expressed as

$$F = Af_{11}\cos\varphi + A^2(f_{20} + f_{22}\cos 2\varphi) + A^3(f_{31}\cos\varphi + f_{33}\cos 3\varphi) + A^4(f_{42}\cos 2\varphi + f_{44}\cos 4\varphi) + O(A^5) \quad (1)$$

The series extends to the fourth order wave amplitude parameter A, with the coefficients f_{mn} functioning as wave-to-force transfer functions. The phase of the linear incident wave is $\varphi = \omega t + \varphi_0$, where $\omega = 2\pi/T_p$ and T_p denote the peak/foundation wave period of the incident waves. The compact term $f_{mn}\cos n\varphi$ signifies $\mathrm{Re}\{f_{mn}e^{i(n\varphi+\psi_{mn})}\}$, with ψ_{mn} representing the phase shift of the force relative to the incident wave at order m and harmonic n. Terms with f_{mm} share the same power of A as the frequency harmonic, while terms with $f_{m(m-2)}$ have an amplitude power two orders higher than the frequency harmonic. Eq. 1 is applicable to regular waves. For simplicity, we illustrate the method for specific focused wave groups within the regular wave framework.

The method described in [1] uses a two-phase method to separate higher harmonics into odd- and even-order components. It involves recording two time histories of a hydrodynamic quantity from interactions with incident waves generated by linear paddle signals that are 180° out of phase. As shown by Eq. 1, the

phase shift causes the signs of the odd harmonics to invert while the even harmonics stay unchanged. Therefore, averaging the difference and sum of the force signals isolates the odd and even harmonics, respectively:

$$\begin{aligned}\frac{(F_0-F_{180})}{2} &= Af_{11}\cos\varphi + A^3(f_{31}\cos\varphi + f_{33}\cos 3\varphi) + O(A^5)\\ \frac{(F_0-F_{180})}{2} &= A^2(f_{20} + f_{22}\cos 2\varphi) + A^4(f_{42}\cos 2\varphi + f_{44}\cos 4\varphi) + O(A^6)\end{aligned} \tag{2}$$

A four-phase method was later introduced in [5], producing additional force signals by introducing additional phase shifts to the paddle motion. This method involves four runs with identical wave-maker signals, in which the Fourier components of the phase-0° wave are shifted by 90°, 180°, and 270°. The resulting forces are labelled as F_0, F_{90}, F_{180}, and F_{270}, and the Hilbert transform is indicated by H, then linear combinations can be used to isolate each harmonic:

$$\begin{aligned}\frac{(F_0-F_{90}^H-F_{180}+F_{270}^H)}{4} &= Af_{11}\cos\varphi + A^3 f_{31}\cos\varphi + O(A^5)\\ \frac{(F_0-F_{90}+F_{180}-F_{270})}{4} &= A^2 f_{22}\cos 2\varphi + A^4 f_{42}\cos 2\varphi + O(A^6)\\ \frac{(F_0+F_{90}^H-F_{180}+F_{270}^H)}{4} &= A^3 f_{33}\cos 3\varphi + O(A^5)\\ \frac{(F_0+F_{90}+F_{180}+F_{270})}{4} &= A^2 f_{20} + A^4 f_{44}\cos 4\varphi + O(A^6)\end{aligned} \tag{3}$$

These combinations sequentially produce the linear (first harmonic) force, the sum of the second and third harmonics, and then the second harmonic difference combined with the sum of the fourth harmonic.

3 RESULTS

Two types of offshore wind turbine platforms are presented in this section.

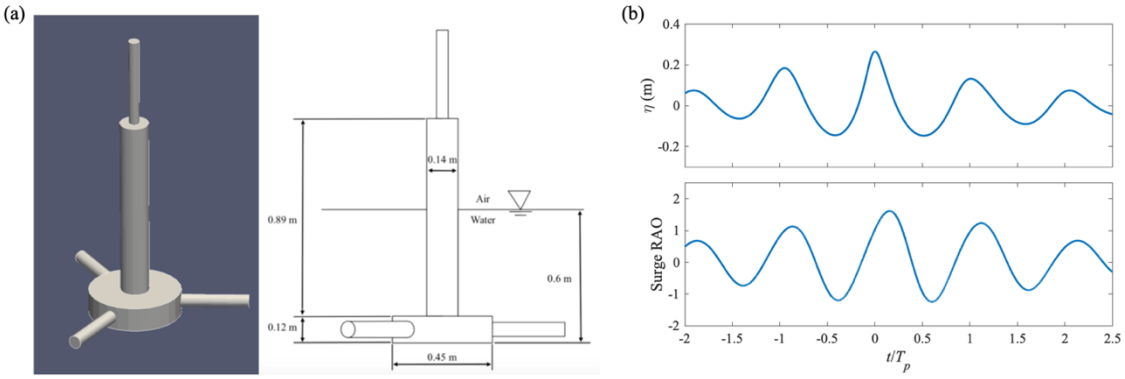

Figure 1: (a) Dimensions of the tension leg platform (TLP), (b) time histories of the free-surface elevation (η) of incident waves at the focal location in an empty tank and the surge RAO (ratio of surge motion to the peak value of η) of the TLP induced by incident waves.

3.1 Tension Leg Platform (TLP)

Fig. 1(a) shows a TLP interacting with a focused wave group depicted in Fig. 1(b). The wave group generated by the JONSWAP spectrum has a peak period of 2.2 s and reaches a maximum wave elevation of 0.27 m at the focal point, in a wave tank with a water depth of 1.2 m. The TLP is equipped with three pre-tensioned mooring lines, each connected to the ends of horizontal legs and anchored to the tank floor.

The linearised mooring stiffness in the surge direction is 86 N/m. Heave motion is ignored due to the high initial vertical axial stiffness of the mooring lines. Pitch and roll movements are minimal, with maximum angles below 1° even under severe conditions, and generally much less than that [6]. Therefore, the analysis focuses only on surge motion. The incident waves caused significant surge displacements, as shown in Fig. 1(b), and no nonlinear effects were observed in the time histories of the surge motion.

This research used CFD simulations, with validation in [6] for the regular wave test cases. The time histories of the forces in Fig. 2(a) show obvious nonlinearities. The two-phase method from Eq. (2) isolates the phase 0° inline force, with separated force amplitude spectra plotted in Fig. 2(a). Each spectrum is transformed back into the time domain using inverse FFT, producing individual harmonic time series shown in Fig. 1(b). To visualise their distribution, envelopes are added: a linear envelope from a Hilbert transform, and envelopes for $n \geq 2$ derived by raising the linear envelope to the nth power and scaling to match measured maxima via least squares. The higher-order harmonics are well captured by the envelopes predicted by the linear force envelopes. Even with significant surge motions, the TLP's force remains consistent with earlier results for a fixed vertical cylinder (i.e., a monopile-type offshore wind turbine foundation) in [1]. The findings confirm that the phase decomposition method remains effective for a floating TLP system.

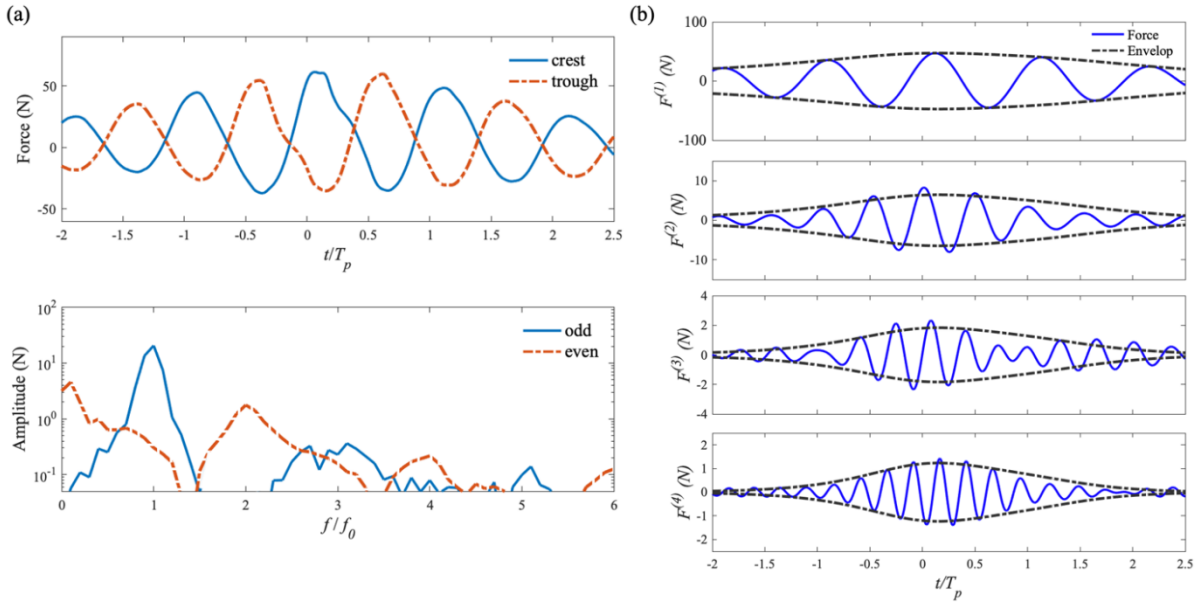

Figure 2: (a) Time histories of the two-phase inline forces obtained by phase-shifting the crest-focused (i.e., phase 0°) inline force generated by the incident waves in fig. 1(b) and force-amplitude spectra separated by the phase-decomposition method, (b) separated individual harmonic inline force from the phase 0° inline total force, $F^{(n)}$ denotes the nth-harmonic force component.

3.2 Truncated Cylinder

Instead of a bottom-mounted cylinder as the monopile foundation of an offshore wind turbine, a truncated cylinder can be regarded as a spar-type platform structure. The study also uses CFD simulations, validated in [7]. Fig. 3(a) illustrates a tilted truncated cylinder with a 20° pitch angle, compared with a vertical cylinder, to assess orientation effects by imposing prescribed static pitch angles during the operations of a spar-type platform. The focused wave group used in this test has a peak wave period T_p of 1.9 s, a wave elevation at the focal point η of 0.24 m, and interacts with the truncated cylinder, which has a radius R of 0.125 m and a draught of 0.5 m, in a wave tank with 0.9 m water depth. The four-phase method from Eq. (3) isolates the phase 0° inline force, as shown in fig. 3(b). After applying the four-phase method, the linear

and fifth-order harmonics appear in the same spectrum, well separated from neighbouring harmonics such as the zeroth (long-wave) and third-order components. Likewise, the second, third, and fourth orders are cleanly isolated in their respective spectra, as shown in Fig. 3(b). Fig. 3(c) shows the separated individual harmonic inline force from the phase 0° inline total force, obtained by the four-phase method. The envelopes are obtained in the same manner as in Fig. 2(b), indicating the same relationships between the higher-order force harmonics and the linear force, and showing that the pitch position will not change these relationships. In the current study, the cylinder is kept rigid and fixed in translation. A spar-type platform with free motion will then be simulated and presented at the workshop.

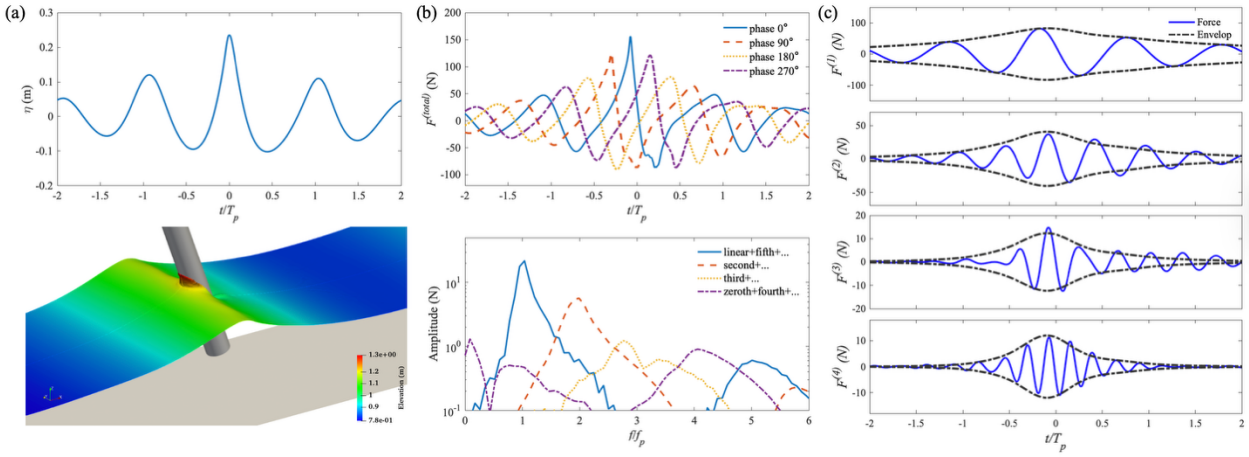

Figure 3: (a) Time histories of the free-surface elevation (η) of incident waves measured at the focal location in an empty tank and the wave interacting with a tilted truncated cylinder, (b) the four-phase inline forces obtained by phase-shifting the crest-focused (i.e., phase 0°) inline force generated by the incident waves in (a) and force-amplitude spectra separated by the phase-decomposition method, (c) inline force harmonic separations using the four-phase method.

4 SUMMARIES

This abstract illustrates the feasibility of the phase-decomposition method across different floating offshore wind turbine platforms. Further nonlinear analysis and findings based on this method will be presented at the workshop.

REFERENCES

[1] Chen, L.F., Zang, J., Taylor, P.H., Sun, L., Morgan, G.C.J., Grice, J., Orszaghova, J., Tello Ruiz, M., 2018. *An experimental decomposition of nonlinear forces on a surface-piercing column: stokes-type expansions of the force harmonics*. J. Fluid Mech. 848, 42–77.

[2] Tang, T., Ryan, G., Ding, H., Chen, X., Zang, J., Taylor, P.H., Adcock, T. A.A., 2024. *A new Gaussian process based model for non-linear wave loading on vertical cylinders*. Coastal Eng. 188, 104427.

[3] Zang, J., Ding, H., Chen, X., Adcock, T. A. A., Tang, T., Hlophe, T., Dai, S., Taylor, P. H. (23 Jun 2025). *SeaSwallowsTool*. University of Bath. Download page: https://www.sea-swallows.org/download

[4] Stokes, G.G., 1847. *On the theory of oscillatory waves*. Trans. Cambridge Philosophical Soc. 8, 441–455.

[5] Fitzgerald, C.J., Taylor, P.H., Eatock Taylor, R., Grice, J., Zang, J., 2014. *Phase manipulation and the harmonic components of ringing forces on a surface-piercing column*. Proc. R. Soc. A: Math. Phys. Eng. Sci. 470.

[6] Ding, H., Chen, Q., Zang, J., 2024. *Numerical simulation of wave interactions with floating offshore renewable energy structures: a comparative study between a particle-based PIC model and OpenFOAM*. J. Fluids Struct. 126, 104092.

[7] Ding, H., Brook-Lawson, J., Buldakov E., Zang, J., 2026. *Nonlinear hydrodynamic forces on a truncated cylindrical offshore wind turbine platform*. Ocean Eng. 343, 123577.